Multimodal Merging of Satellite Imagery with Meteorological and Power Plant Data in Deep Convolutional Neural Network for Short-Term Solar Energy Prediction

Gwangjoong Kim (1), Hunsoo Song (1), Minho Kim (1), Yongil Kim (1)

[1] Seoul National Univ., 1 Gwanak-ro, Gwanak-gu, Seoul 08826, Korea
Email: todayfirst@snu.ac.kr; songhunsoo92@gmail.com; mhk93@snu.ac.kr; yik@snu.ac.kr

KEY WORDS: Solar Energy Prediction, Convolutional Neural Network, Meteorological Satellite Imagery, Photovoltaics (PV) System, PV Prediction

ABSTRACT: Solar energy is a promising renewable energy source, but stable generation of photovoltaic (PV) power is largely impaired by meteorological phenomena. Ground-based weather measurements are limited in their ability to fully capture the unpredictable nature of meteorological conditions. However, remotely-sensed satellite imagery can offer crucial information on the atmosphere and the local environment, providing a broader perspective for more accurate PV estimation. This study proposes a novel Deep Convolutional Network (DCNN) framework, which integrates meteorological satellite imagery, meteorological elements, and past PV measurements to predict short-term PV power. The performance of the proposed model for solar energy prediction was tested on a solar power plant located in South Korea. Results demonstrated that the DCNN model successfully learned the complex meteorological factors such as cloud motion and solar irradiance by integrating stacked multi-temporal COMS images with ground-based meteorological data and previous PV data as input sources. In addition, we confirmed that the use of multi-temporal, multi-band meteorological satellite image significantly improves the prediction accuracy. These results were confirmed by evaluating the normalized mean absolute error of the solar energy output which indicated the proposed model's effectiveness for short-term PV power predictions.

1. INTRODUCTION

Solar energy has emerged as a significant renewable resource for future sustainable development (Ghosh and Rahman, 2016; Wan et al., 2015). However, the generation of solar photovoltaic (PV) power from solar power plants can fluctuate over time, due to the continuously changing nature of meteorological phenomena and cloud coverage. In more detail, the efficiency of PV output can be influenced by numerous meteorological factors such as solar irradiance, cloud movement, cloud coverage, and other weather conditions which continuously differ over time (Voyant et al., 2017; Alfadda et al., 2018; Fu et al., 2013; Hosenuzzaman et al., 2015). Understanding these meteorological factors is therefore paramount to predict the generated PV output, particularly when such information is required for services that distribute the harnessed PV energy.

In general, ground-based weather measurements are commonly utilized to interpret the meteorological factors, ground, but application of these methods alone cannot fully capture the variable nature of meteorological

conditions. This shortcoming arises because these measurements only represent conditions with respect to present time and for the local environment. Alternatively, remote sensing methods using satellite images can offer crucial information of the atmosphere as well as interactions affecting the local environment by utilizing wider coverage areas for more accurate PV power prediction.

In literature, previous studies have performed PV power prediction via remote sensing methods focusing on ground-based sky imager and meteorological satellite imagery. Ground-based sky imagers have been used to predict cloud motion efficiently, thereby generating solar irradiance and PV estimation (Fu et al., 2013). However, ground-based sky imagers are restricted to a small range in coverage and only RGB channels (bands), which ultimately restricts its forecasting time to intra-hour and limits the imagers from obtaining essential atmospheric features. On the other hand, meteorological satellites have exhibited the potential to capture a greater degree of information on the atmosphere and the local environment given with their wider coverage of observation and broader spectral resolution using a greater number of spectral bands. Although meteorological satellites can compensate for the shortcomings of ground-based sky imagers, these satellites are limited by its coarse spatial resolution, which makes it difficult to identify small-scale variations of atmospheric conditions in detail (Wolff et al., 2016; Alfadda et al., 2017; Massida et al., 2018; Almeida et al., 2017; Chow et al., 2016).

Moreover, the power plant capacity and PV cell characteristics also impact PV generation (Wan et al., 2015). The former factor refers to the output encompassing the conversion from solar energy harnessed at the PV cell to the electricity generated at the power plant. With regards to the latter of these factors, PV generation is influenced by the PV cell's total size, material type of the panel, panel's standing angle with respect to the sun, and solar altitude. In addition, meteorological elements such as sun elevation and zenith angle are also considered because they significantly affect the performance of PV prediction, but cannot be derived from the features mentioned above.

Since various features should be considered together for PV prediction, many studies have attempted to perform PV prediction using a machine learning based method (Voyant, 2017). For instance, Alfadda (2017) attempted to predict short-term PV output using a support vector machine (SVM) based method. Other studies incorporated numerous factors such as temperature, module temperature, solar irradiance, wind velocity, and PV power. Gandelli (2014) proposed artificial neural network (ANN) based method and used weather temperature, wind speed, humidity, pressure, and cloud cover, while Massidda (2018) used gradient-boosted regression trees fed by numerical weather forecasts, astronomical data, and global horizontal irradiation. However, in the majority of these studies, these factors rely on measurements taken locally which may not be in the vicinity of the studied solar power plant location. In addition, few studies have assessed the effectiveness of using meteorological satellite imagery as input datasets for PV prediction.

To address these aforementioned limitations, we propose a Deep Convolutional Neural Network (DCNN) framework which can exploit various input features to predict PV output effectively. To evaluate the performance of our proposed approach, the framework was tested on a solar power plant located in Jeungpyeong, South Korea. We introduced meteorological satellite images, past hourly PV output data, solar zenith angle, azimuth angle, and time in hours as input features for the framework. To efficiently learn the features of the meteorological satellite images, we varied the input satellite image by small patch sizes and used multi-temporal satellite images, stacked with visible and infra-red band images as well as a post-processed insolation product.

The present study is structured in the following order: Section 2 provides the Jeungpyeong solar power plant locations as well as the multiple factors, including specifications of the meteorological satellite imagery used in this study. Section 3 introduces our proposed DCNN framework for PV prediction and describes the model's architecture and workflow. Section 4 outlines and analyzes the experimental results based on the various tests using our proposed approach. The last section provides a summative review of this study and offers suggestions for future work and improvements for more effective PV forecast methods.

2. STUDY AREAS AND DATASET

2.1 Jeungpyeong Solar Power Plant

In this paper, the study area is focused on predicting the PV output from a solar power plant located in Jeungpyeong (36.796303˚N, 127.594515˚E), in Chungcheongbuk-do province of South Korea. The maximum capacity of the plant is 993kW per hour. The precise location of the solar power plant is shown in Figure 1.

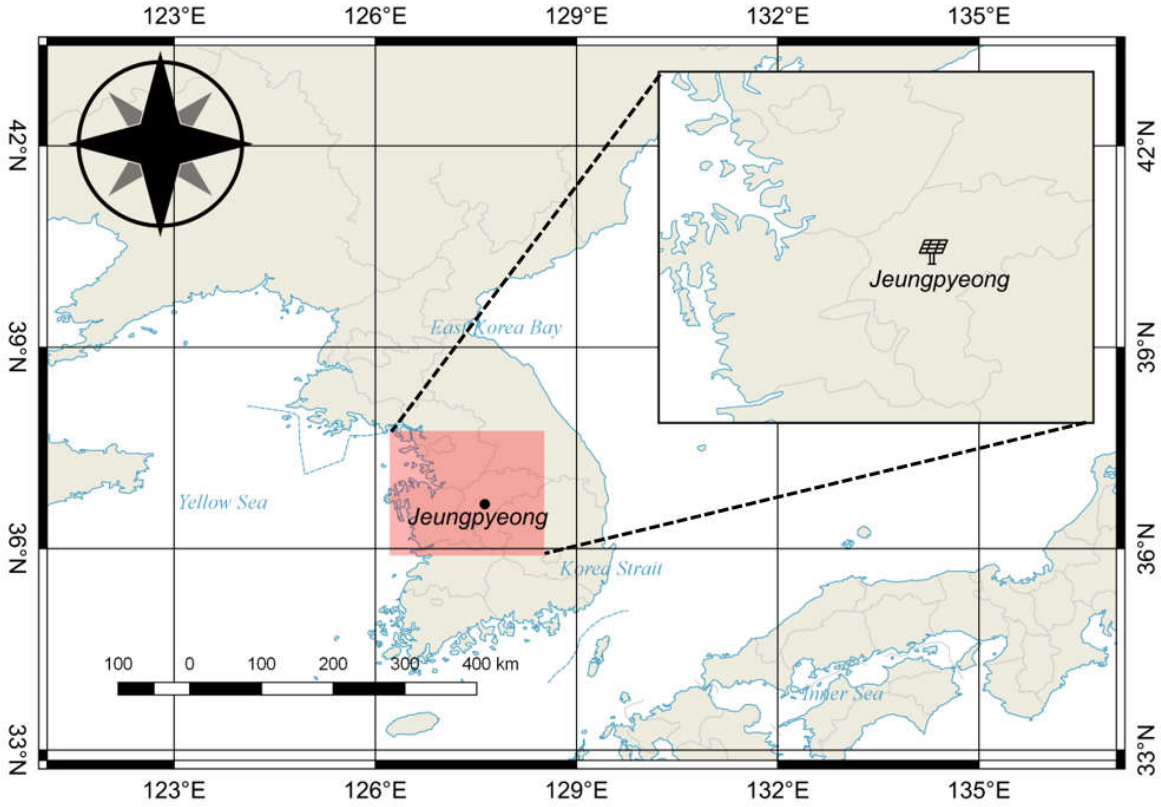

Figure 1. Location of study area and Jeungpyeong solar power plant.

2.2 Meteorological Satellite Imagery

For this study, Communication, Ocean, and Meteorological Satellite (COMS) was used as input satellite imagery. COMS was Korea's first geostationary multi-purpose satellite, stationed at an altitude of 36,000 km above the Earth's equator and at a longitude of 128.2°E. The satellite is responsible for ocean color monitoring and meteorological observations for the Korean peninsula. Image acquisitions of the study area were taken from

the Meteorological Imager (MI) sensor module aboard COMS. The sensor uses 5 channels (1 visible and 4 infrared bands) and provides imagery every 15 minutes. Images were acquired from National Meteorological Satellite Center (NMSC), which provides level-1 COMS imagery for the bands shown in Table 1 as well as 16 different level-2 products, which are generated as a composite of different band inputs from the level-1B COMS data and auxiliary data through the COMS Meteorological Data Processing System (CMDPS). The level-2 products are subsequently applied in weather forecasts, numerical forecasts, and climate change predictions. From the list of level-2 images, we selected the "Insolation" (INS) products as one of the inputs for our model because the level of insolation demonstrated relatively high level of correlation with other input datasets described in the following sub-section below.

Table 1. Specifications and applications for COMS MI images (NMSC, 2019)

Band	Wavelength (μm)	Applications
Visible (VIS)	0.55 - 0.80	Cloud coverage, atmospheric motion vector, fog, Asian dust
Shortwave Infrared	3.5 - 4.0	Land surface temperature, night fog, low-level clouds
Water Vapor	6.5 - 7.0	Mid-upper atmospheric humidity, upper atmospheric motion
Infrared-1 (IR1)	10.3 - 11.3	Cloud information, sea surface temperature, Asian dust
Infrared-2 (IR2)	11.5 - 12.5	

2.3 Other Datasets

Apart from COMS imagery, other input datasets in this research include past hourly PV output data, time (in hours), azimuth angle, and solar elevation. The applicable time for prediction was filtered from 6AM to 8PM, considering the times for sunrise and sundown. Past PV output data were obtained from April 1st, 2018 to March 31st 2019 for the Jeungpyeong power plant. With regards to azimuth angle and elevation data, refer to Figure 2. Suppose for PV prediction at a given hour "n", the colored segment represents the generated PV between "n-1" and "n" hours. Based on this principle, azimuth angle and elevation data should be more effectively represented by intervals rather than by discrete points (per hour). While the other features were inputted in hourly time-stamps, the azimuth angle and elevation datasets were therefore divided within an hour into four 20 minute intervals.

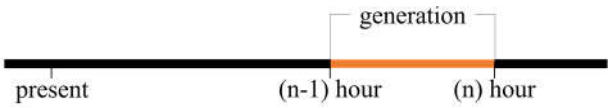

Figure 2. Visual explanation for dividing azimuth angle and elevation data into intervals.

3. DCNN FRAMEWORK FOR PV FORECAST

In this study, we propose a DCNN framework for PV output prediction, as illustrated by the overall workflow given in Figure 3. In principle, the convolutional layers first extract features from multi-temporal COMS image patches. Features from the convolutional layers as well as the other non-image features are concatenated together, and this "stack" of features is then converted into fully connected layers to generate PV predictions. With regards to the DCNN model, 20 days, out of a year, were selected randomly to serve as test data, while 20 percent of the training data was used as validation data to evaluate the model.

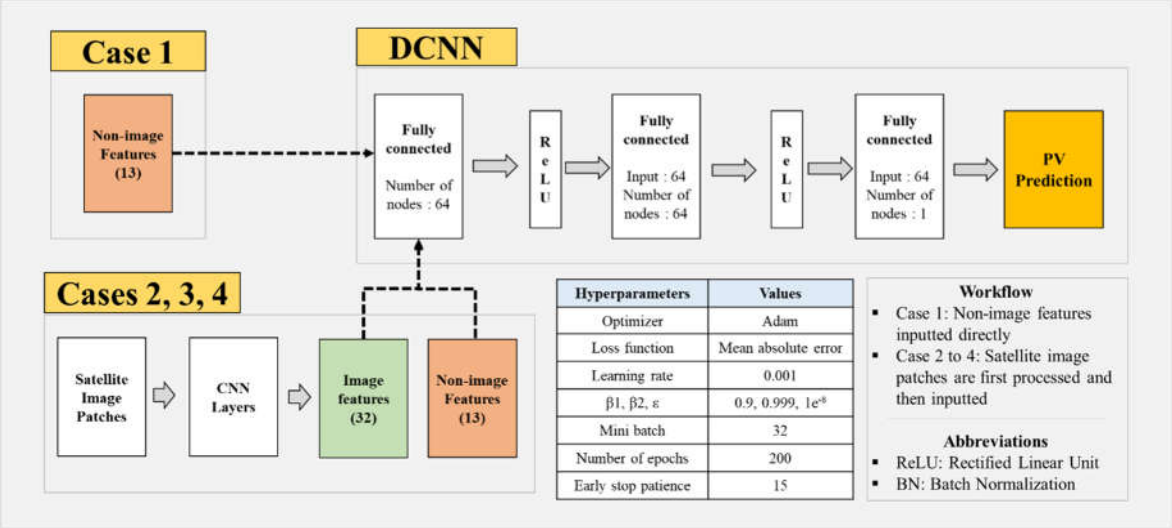

Figure 3. Workflow of proposed DCNN framework.

The proposed DCNN uses COMS imagery, time (in hours), zenith angle, elevation, and past hourly PV output data as input features. Based on these input features, various tests were constructed to evaluate the DCNN model. Case 1 used only 13 non-image features for input datasets, which included past PV output data (0h, -1h, -2h, -3h), azimuth angle, elevation, and time (in hours). For Cases 2 to 4, COMS images were utilized at different time intervals (0h, -1h, -2h, -3h) and in varying patch sizes. To elaborate, Case 2 used 3-by-3 sized COMS patches and two convolutional layers, Case 3 used 5-by-5 sized COMS patches and four convolutional layers, and lastly, Case 4 used 7-by-7 sized COMS patches and five convolutional layers. The different setups of input datasets were then processed with the 13 non-image features (identical features used for Case 1) into the fully connected layers to generate PV prediction results, as shown in the top-right diagram in Figure 3. The different setups of Cases 2 to 4 using multitemporal COMS images are shown in Figure 4.

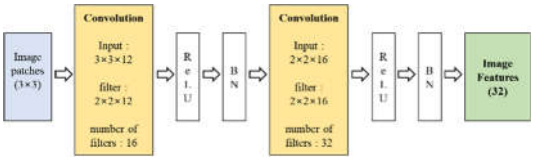

(a) Case 2

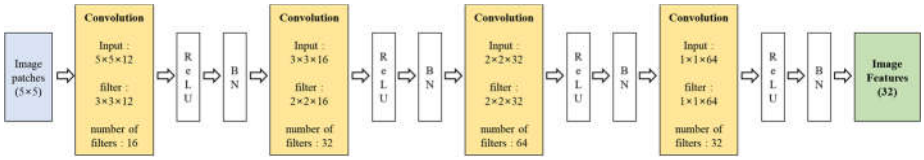

(b) Case 3

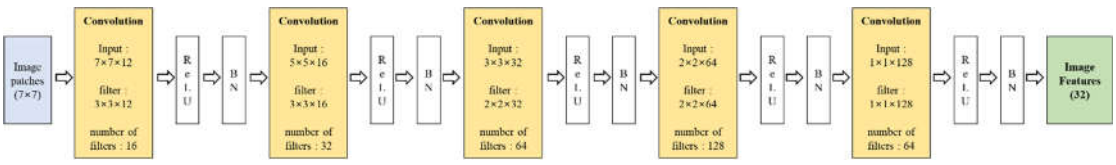

(c) Case 4

Figure 4. Test cases for proposed DCNN framework utilizing COMS image patches as input features.

4. EXPERIMENTAL RESULTS AND DISCUSSION

Since the neural network is initialized with random values and the order of the training data is also random, results from evaluation metrics can vary despite using the same training dataset and network structure. In light of this issue, 30 iterations were conducted for each case and evaluated using the Normalized Mean Absolute Error (nMAE) and correlation coefficients (CC). The formula for both metrics are displayed in Table 2.

Table 2. Performance evaluation metrics used in this study

Metric	Formula
Normalized Mean Absolute Error (nMAE)	$NMAE(\%) = \frac{1}{N}\sum_{t=1}^{N}\frac{abs(meas - pred)}{capacity}$
Correlation Coefficient (CC)	$CC = \frac{\sum_{t=1}^{N}(meas - meas_{mean})(pred - pred_{mean})}{\sqrt{(\sum_{t=1}^{N}(meas - meas_{mean})^2\,(\sum_{t=1}^{N}(pred - pred_{mean})^2)}}$

The average nMAE and standard deviation following 30 iterations of the prediction results using the test data are shown in Table 3 for each case. Comparing Case 1 with Cases 2 to 4, the results demonstrate that, in general, the use of multitemporal COMS images decreased the average nMAE levels. The average improvement of nMAE was found to be 0.51%. Moreover, larger patch sizes showed a tendency to decrease the standard deviation of nMAE from Cases 2 to 4. In particular, Case 3, which used a patch size of 5-by-5 and four convolutional layers, returned the best performance results in terms of average nMAE levels.

Table 3. Average and standard deviation of nMAE

nMAE Statistic	Case 1	Case 2	Case 3	Case 4
Average	5.77%	5.26%	5.21%	5.30%
Standard deviation	0.19%	0.38%	0.32%	0.24%

The PV output estimates produced using the proposed DCNN approach were plotted for each case with respect to true values of PV output recorded two-hours in advance at the Jeungpyeong solar power plant. The CC of each case is shown in Figure 5. On the one hand, the overall high CC levels highlighted the superiority of deep learning methods and the effective selection of the input features used in this study. On the other hand, when considering the addition of COMS images, Cases 2 to 4 showed a slight increase in CC in comparison to Case 1.

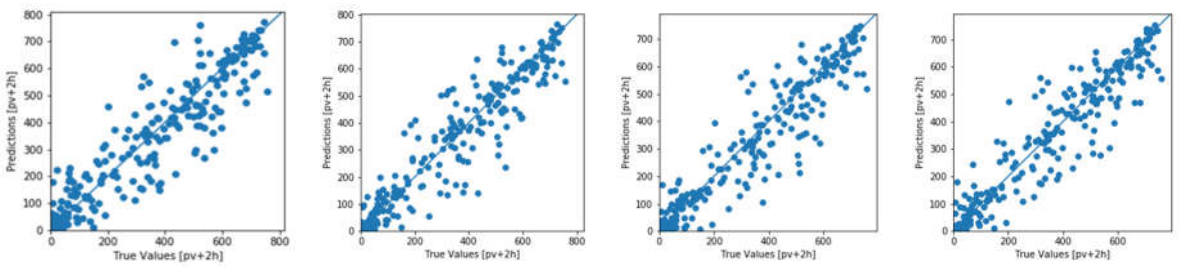

(a) Case 1 (0.9445) (b) Case 2 (0.9545) (c) Case 3 (0.9584) (d) Case 4 (0.9570)

Figure 5. Correlation of PV predictions using the proposed DCNN framework with actual PV output values. Each case is illustrated using a regression plot with corresponding correlation coefficients.

From the results of each case, Case 3 returned the lowest average nMAE and the highest CC. Based on this reasoning, the results suggested that the integration of meteorological satellite images and products can help to reduce the error in PV predictions. In particular, using COMS can also help to take into account unfavorable scene conditions such as obstructing cloud coverage. The following graphs in Figure 6 shows the true PV output (reference value), the predicted PV output using the proposed DCNN framework, and the normalized absolute error. These plots were taken based on image acquired in clear sky conditions.

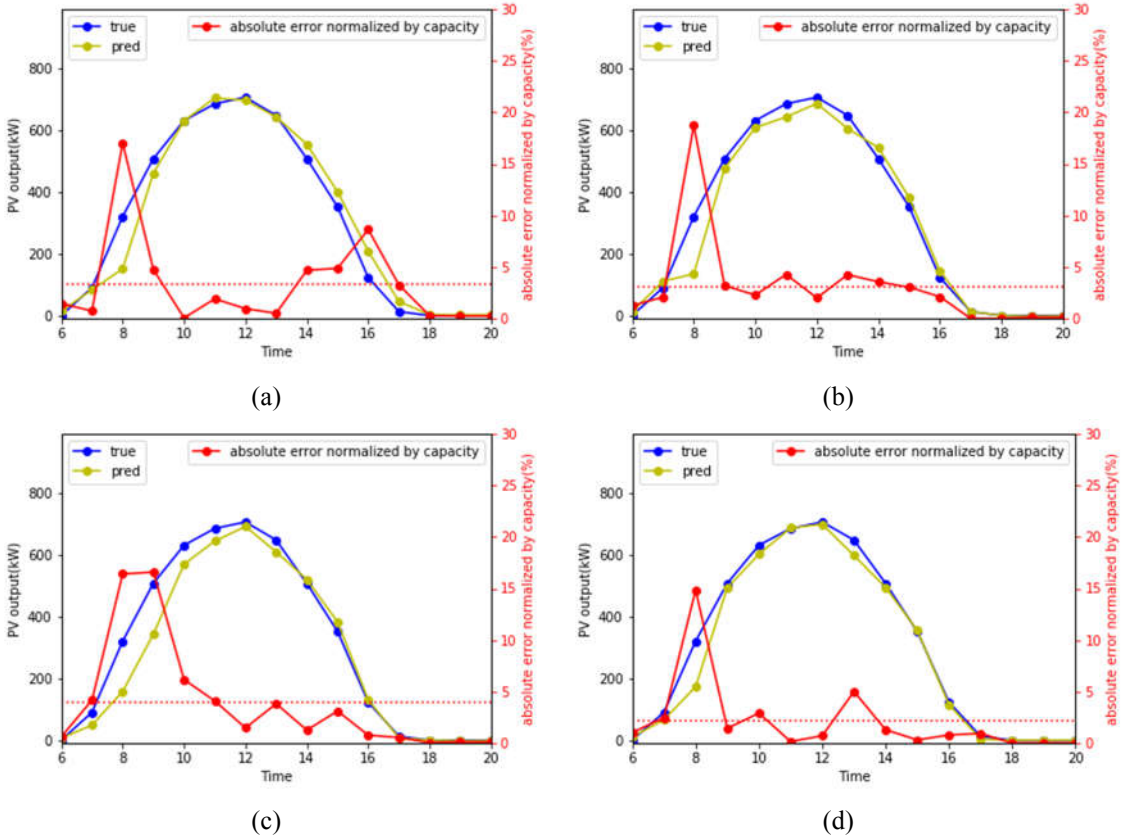

Figure 6. PV output distributions under clear sky conditions. Plot distributions (a) to (d) represent Cases 1 to 4, respectively. The predicted and actual PV output plots correspond to the left axis while the dotted line denoting "absolute error normalized by capacity" corresponds to the right axis.

In clear sky conditions, all cases produce a very low level of nMAE of around 3 to 4 %. Although clear sky conditions are ideal for PV output forecasts, such conditions are not always guaranteed. Instead, unideal conditions need to be considered as well. In other words, when the sky is not fully clear due to cloud coverage or unfavorable weather conditions, the amount of PV generation can become irregular. For such conditions, this issue is reflected by an overall increase in error in all four cases. However, the increase in error using satellite imagery is smaller than the case without using satellite imagery. The following distributions organized in Figure 7 show the results of two different scenes that are both influenced by cloud coverage.

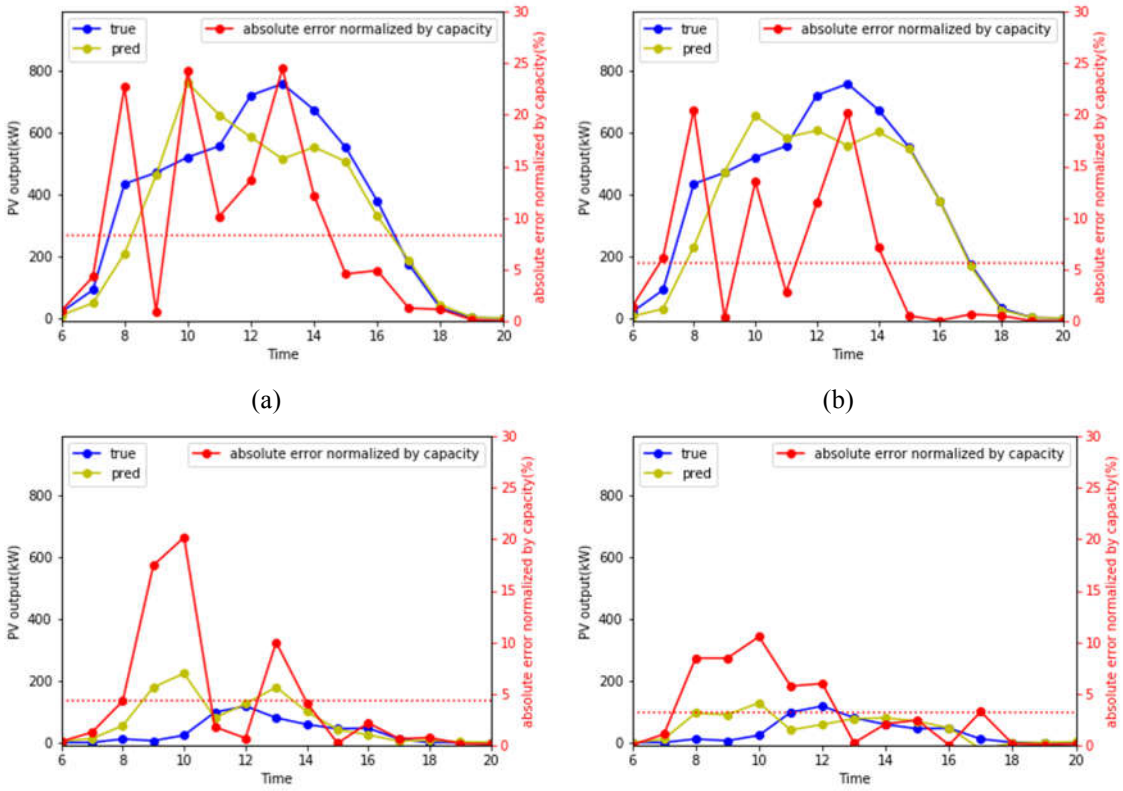

Figure 7. Comparison of PV output results under unfavorable conditions. (a) and (c) depict two different results from Case 1, while (b) and (d) display the corresponding results from the most accurate and correlated scenario (Case 3). The plots in this figure correspond to the same axes as that of Figure 6.

Although satellite images were included to enrichen the performance of the proposed DCNN framework, a margin of error in resulting PV predictions is still present. First, the accuracy of PV forecasts can be affected by seasonal variation in the data. Second, the inherent limitations of satellite imagery can influence the accuracy of PV predictions as well. Since the spatial resolution of COMS MI is 1 km (for VIS bands), this specific resolution may be insufficient to detect smaller clouds or meteorological elements. In the case of using level-2 COMS INS data, the accessed datasets include permanently modified lines that demarcate administrative boundaries in the Korean peninsula. These lines add confusion to the DCNN model and can affect the accuracy of the PV output prediction. Third, unpredictable nature of meteorological conditions and cloud motion, as well as cloud generation and dissipation, can also affect the accuracy of PV estimation. Fourth, both Figure 6 and 7 exhibit the relatively large levels of error observed for values between 8AM and 10AM in the morning. To compensate for this shortcoming, additional data acquired at dawn would be required to effectively predict the amount of power generated at this time.

5. CONCLUSION

In this study, we proposed a DCNN framework which incorporates past hourly PV output data, finely-separated azimuth angle and elevation datasets, time (in hours), and multi-temporally acquired COMS images

for short-term (2-hour ahead) PV output predictions. The proposed approach consisted of four cases of which one used 13 non-image features as input, while the remaining three cases incorporated COMS images at varied image patch sizes and number of convolutional layers. In other words, the DCNN model was compared with a DNN that used only non-image features as input data. From the experimental results, the proposed DCNN approach generated PV output estimates two hours in advance to a considerably high level of accuracy and revealed a strong correlation with respect to actual PV values recorded at the Jeungpyeong solar power plant. To elaborate further, the PV output predictions from all test cases displayed strong correlation of CC values greater than 0.95 with respect to actual PV data. Furthermore, the input setups which used satellite imagery (Cases 2 to 4) demonstrated higher nMAE and CC values than the DNN case (Case 1). In particular, Case 3 which used 5-by-5 patch size and four convolutional layers, returned the best level of performance with an average nMAE of 5.21%. However, the proposed framework is also affected by various error sources. In order to improve the performance of this approach and to enhance the accuracy of PV output forecasts, future studies should focus on the selection of optimal input features. Moreover, in order to take into account, the seasonal changes and to better reflect the factors influencing PV output, adding average PV output or other relevant weather factors as input features can be considered. Lastly, using the skip connection or inception and a pre-trained network are also other noteworthy options that can improve the effectiveness behind the learning process of the DCNN model.

ACKNOWLEDGMENT

The authors gratefully acknowledge SK Telecom for sponsoring this research and the National Meteorological Satellite Center for supplying COMS images.

REFERENCES

Alfadda, A., Adhikari, R., Kuzlu, M., and Rahman, S., 2017. Hour-ahead solar PV power forecasting using SVR based approach. 2017 IEEE Power & Energy Society Innovative Smart Grid Technologies Conference (ISGT), pp. 1-5.

Alfadda, A., Rahman, S., and Pipattanasomporn, M., 2018. Solar irradiance forecast using aerosols measurements: A data driven approach. Solar Energy, 170, pp. 924-939.

Almeida, M., Muñoz, M., de la Parra, I., and Perpiñán, O., 2017. Comparative study of PV power forecast using parametric and nonparametric PV models. Solar Energy, 155, pp. 854-866.

Fu, C. L., and Cheng, H. Y., 2013. Predicting solar irradiance with all-sky image features via regression. Solar Energy, 97, pp. 537-550.

Gandelli, A., Grimaccia, F., Leva, S., Mussetta, M., & Ogliari, E., 2014. Hybrid model analysis and validation for PV energy production forecasting. 2014 International Joint Conference on Neural Networks (IJCNN), pp. 1957-1962.

Ghosh S. and Rahman S., 2017. Global deployment of solar photovoltaics: Its opportunities and challenges. In Proc. 2016 IEEE PES Innovative Smart Grid Technologies Conf., pp. 1-6.

Hosenuzzaman, M., Rahim, N. A., Selvaraj, J., Hasanuzzaman, M., Malek, A. A., and Nahar, A., 2015. Global prospects, progress, policies, and environmental impact of solar photovoltaic power generation. Renewable and

Sustainable Energy Reviews, 41, pp. 284-297.

Kingma, D. P., and Ba, J., 2014. Adam: A method for stochastic optimization. arXiv:1412.6980.

Massidda, L., & Marrocu, M., 2018. Quantile Regression Post-Processing of Weather Forecast for Short-Term Solar Power Probabilistic Forecasting. Energies, 11 (7), pp. 1763.

NMSC (National Meteorological Satellite Center) of Korea Meteorological Administration, Introduction of COMS (Communication, Ocean and Meteorological Satellite), Retrieved September 7, 2019, from http://203.247.66.167/html/homepage/en/ver2/static/selectStaticPage.do?view=satellites.coms.choll_info

Rowlands, I. H., Kemery, B. P., & Beausoleil-Morrison, I., 2011. Optimal solar-PV tilt angle and azimuth: An Ontario (Canada) case-study. Energy Policy, 39(3), pp. 1397-1409.

Voyant, C., Notton, G., Kalogirou, S., Nivet, M. L., Paoli, C., Motte, F., and Fouilloy, A., 2017. Machine learning methods for solar radiation forecasting: A review. Renewable Energy, 105, pp. 569-582.

Wan, C., Zhao, Song, J. Y., Xu, Z., Lin, J., and Hu, Z., 2015. Photovoltaic and solar power forecasting for smart grid energy management. CSEE Journal of Power and Energy Systems, vol. 1 (4), pp. 38-46.

Wolff, B., Kühnert, J., Lorenz, E., Kramer, O., and Heinemann, D., 2016. Comparing support vector regression for PV power forecasting to a physical modeling approach using measurement, numerical weather prediction, and cloud motion data. Solar Energy, 135, pp. 197-208.